

# Synthesis and characterization of chitosan–copper nanocomposites and their fungicidal activity against two sclerotia-forming plant pathogenic fungi

Margarita S. Rubina<sup>3</sup> · Alexander Yu. Vasil'kov<sup>3</sup> · Alexander V. Naumkin<sup>3</sup> · Eleonora V. Shtykova<sup>5</sup> · Sergey S. Abramchuk<sup>3</sup> · Mousa A. Alghuthaymi<sup>4</sup> · Kamel A. Abd-Elsalam<sup>1,2</sup>

Received: 16 May 2017 / Accepted: 11 July 2017 / Published online: 21 July 2017  
© The Author(s) 2017. This article is an open access publication

**Abstract** In this report, the metal-vapor synthesis (MVS) was used for the preparation of copper nanoparticles which was then used for the preparation of chitosan–copper nanocomposite. The antifungal activity of Cu@Chit NCs against two sclerotium-forming plant pathogenic fungi *Sclerotium rolfsii* (*S. rolfsii*) and *Rhizoctonia solani* (*R. solani*) AG-4 was evaluated in vitro and their effects on hyphal morphology, and sclerotia formation were observed for the first time. The NCs were prepared through impregnation of chitosan with colloid solution of copper nanoparticles in organic solvent (acetone or toluene). Transmission electron microscopy shows that the particles have predominantly spherical form, polydisperse character, the mean diameter about 2–3 nm and a rather uniform distribution in the chitosan matrix. Analysis of the small angle scattering curves suggests that the copper particles in the NCs with the size of  $\leq 2$  nm are mostly located in the chitosan pores with the same size. The effect of Cu@Chit NCs on fungal growth reveals some significant inhibitory activity against two tested fungi. The highest level of

inhibition against *S. rolfsii* and *R. solani* AG-4 was observed using the high concentrations of Cu@Chit NC prepared using acetone as a solvent. A loss of the cytoplasm content, cytoplasmic coagulation, irregular shape of mycelia, or destruction in the hyphae was confirmed. The experiments demonstrate that the Cu@Chit NC synthesized via MVS using acetone was more effective than that of toluene in inhibiting fungal hyphae growth against *R. solani* AG-4 and *S. rolfsii*. The results show that the Cu@Chit NCs are fungicidal against both the tested fungus at high concentrations and the fungicidal or fungistatic activity is dependent on the tested fungus species.

**Keywords** Antifungal · Metallic nanocomposites · Copper nanoparticles · Metal-vapor synthesis · *Sclerotium rolfsii* · *Rhizoctonia solani*

## Introduction

One of the most critical issues in the face of mankind is the solution search in the fight against pathogenic microorganisms. This issue now is well visible in the agriculture. A number of different pathogenic fungi and bacteria cause the plant diseases. To solve this problem, the synthetic organic or inorganic pesticides treatment of seeds, plants and crops is widely applied. However, other problems are often emerging. It is well known that chemical agriculture pesticides tend to accumulate in soil causing poisoning, gather in plants and crops, have toxic effect on ecology and sometimes has poor efficacy against some types of microorganisms. Copper compounds are well known as biocide from XVIII century. Nevertheless, the same problems with their usage exist. To enhance antifungal activity

✉ Kamel A. Abd-Elsalam  
kamelabdelsalam@gmail.com

<sup>1</sup> Plant Pathology Research Institute, Agricultural Research Center (ARC), Giza, Egypt

<sup>2</sup> Unit of Excellence in Nano-Molecular Plant Pathology Research Center, Plant Pathology Research Institute, Giza, Egypt

<sup>3</sup> A.N. Nesmeyanov Institute of Organoelement Compounds (INEOS), Russian Academy of Sciences, Moscow, Russia

<sup>4</sup> Biology Department, Science and Humanities College, Shaqra University, Alquwayyah, Saudi Arabia

<sup>5</sup> A.V. Shubnikov Institute of Crystallography, Russian Academy of Sciences, Moscow, Russia

and decrease environmental toxic effect, it is important to develop novel type of biocides [1, 2].

Chitosan is a biodegradable, non-toxic and biocompatible polymer obtained from partly deacetylation procedure of chitin sources. This polymer possesses unique number of biological properties such as antibacterial, antiviral and antifungal activities. Chitosan is established to exhibit the inhibition activity on different stages namely mycelia growth, sporulation, spore viability and germination, and the production of fungal virulence factors [3]. Chitosan and chitosan-based composites in the forms of powders, suspensions, film coatings, scaffolds, and capsules are utilized for crop protection and for increasing resistance of host plants [4]. The using of chitosan in agriculture is possible not only in crop protection of healthy plants but also in plant diseases control [5]. Although exact mechanisms of the chitosan inhibition have not been sufficiently studied, it is assumed that chitosan can act as chelating agent for minerals and nutrients of pathogens thus leading to their death [6]. It is known that chitosan antifungal activity depends on different factors like degree of acetylation, concentration, form of usage, type of target organism and molecular weight [7]. Numerous studies are dedicated to investigation of such correlations. Because of the large number of  $\text{NH}_2$ - and  $\text{OH}$ - in chitosans chemical structure, chitosan can be used as effective anchoring agent for metal nanoparticles (NPs). Cu NPs have pronounced bactericidal properties against various types of organisms [8]. The improved antimicrobial activity of Cu NPs as compared to copper salt is due to their unique property, i.e., large surface area to volume ratio [9]. Recently, the investigations showed that incorporation of Cu NPs into chitosan matrix significantly enhanced its antimicrobial and antifungal activity [10–13]. The Cu@Chit NCs can combine the properties of biopolymer and nanosized copper; therefore, their application can be more effective than separately.

Insertion of NPs into chitosan matrix can be done by different ways. The most versatile methods are based on reduction of metal salts with the presence of stabilizing and reducing agents in the water medium. The chemical reduction method is applied for synthesis of a huge number of different NPs including Cu NPs. Because of the high tendency of Cu NPs to be oxidized, it is a big issue to prepare copper in a zero-valent state.

One of the promising methods for preparing colloidal NPs solutions and their based metal–polymer NCs is metal-vapor synthesis (MVS). This cryochemical method is based on metal evaporating under  $p = 10^{-4}$ – $10^{-6}$  Torr and  $T = 77$  K and following co-condensation process with organic ligand/solvent on the walls of quartz reactor. The resulting cryomatrix upon being heated forms the colloidal solution of NPs in organic solvent called as organosol. To prepare composites with metal NPs, the different

kinds of supports (organic/inorganic) are impregnated with organosol. MVS technique is well-proven and effective route to make composites with tailored magnetic, antibacterial, and catalytic properties. The MVS efficacy for preparing biopolymers and their hybrids with biologically active metal NPs has already been demonstrated [14–16].

This work is dedicated to the fabrication of Cu@Chit NCs and testing these materials against two sclerotium-forming plant pathogenic fungi *R. solani* AG-4 and *S. rolfisii*. To obtain metal-biopolymer NCs the original cryochemical technique will be employed.

## Experimental part

### Materials and reagents

Toluene and acetone with special purity grade, 99.5% were used as the solvents for MVS. Prior to synthesis toluene was dried over Na and acetone was dried under molecular sieves (4 Å) then solvents were degassed in vacuum of  $10^{-1}$  Pa by freezing–thawing cycles. The metal source was Cu foils (99.99%) whose surface was pre-treated with concentrated  $\text{HNO}_3$  and distilled  $\text{H}_2\text{O}$  to eliminate oxide films. Chitosan (CAS 9012-76-4) with the molecular weight of 310–375 kDa and degree of deacetylation  $\geq 75\%$  was purchased from Aldrich. Before the impregnation procedure chitosan powder was degassed for 12 h under vacuum of  $10^{-1}$  Pa at 40 °C.

### Preparation of Cu@Chit nanocomposites

The metal-vapor technique was used for the preparation of copper-carrying chitosan NCs. The full preparing procedure can be divided into the main three steps. In the first step, we obtained the NPs colloidal solution in organic solvent referred as organosol. In this work the copper-acetone and copper-toluene organosol were prepared. For this purpose 0.26 g of copper foil (about 200  $\mu\text{m}$  thickness) were evaporated by resistively heating a tantalum boat ( $l = 90$  mm,  $b = 5$  mm) at a residual pressure of  $10^{-5}$  Torr and co-condensed with 120 mL of solvent on liquid nitrogen-cooled walls of a 5 L reactor. The second step was the impregnation of chitosan powder with organosol. On this step the frozen matrix was melted and the organosol was infiltrated into chitosan powder in an evacuated Schlenk vessel. The black organosol was instantly discolored and the embedding of chitosan with metal NPs was occurred immediately. More detailed information about MVS set up and procedure reported elsewhere [17]. On the third step, the solvent was removed and the metal-carrying chitosan powder was dried in a vacuum of 1 Pa at 60 °C



during 3 h. All manipulations were performed in a pure Ar atmosphere. The Cu@Chit NCs obtained by means of Cu-acetone and Cu-toluene impregnation are referred as Cu@Chit-1 and Cu@Chit-2, respectively.

### Characterization of Cu@Chit nanocomposites

#### X-Ray fluorescence analysis (XRF)

Cu concentration (%wt) in the samples was measured with a VRA 30 X-ray fluorescent analyzer (Germany) using the M K $\alpha$  line of the X-ray fluorescence spectrum. In order to excite XF, X-ray tube with a Mo anode was used in the 50 kV, 20  $\mu$ A regime. Cu@Chit NCs were analyzed as pressed pills.

#### Transmission electron microscopy (TEM)

TEM microphotographs were performed using a transmission electron microscope LEO 912AB OMEGA, Zeiss (Germany) at acceleration voltage of 100 kV. The Cu-carrying chitosan powder was previously suspended in deionized water (18 M $\Omega$ ) and sonicated in the ultrasonic bath during 15 min. Then, a small amount of the suspension was dripped onto a copper mesh covered with formvar film.

#### Small-angle X-ray scattering (SAXS)

Conventional small-angle X-ray scattering (SAXS) measurements were performed using a laboratory diffractometer “AMUR-K” (Institute of Crystallography, Moscow) at a wavelength  $\lambda = 0.1542$  nm with a Kratky-type (infinitely long slit) geometry covered the range of momentum transfer  $0.12 < s < 6.0$  nm $^{-1}$  (here,  $s = 4\pi \sin\theta/\lambda$ , where  $2\theta$  is the scattering angle). The scattering curves were corrected for the background scattering and primarily processed using standard procedures and program PRIMUS [18].

Size distributions of heterogeneities presented in the specimens and those of Cu nanoparticles were computed using the indirect transform program GNOM [19]. Assuming the particles to be spherical, the program solves integral equation:

$$I(s) = \int_0^{\infty} D_V(R) m^2(R) i_0(sR) dR,$$

where  $I(s)$  is scattering intensity,  $R$  is the radius of a sphere,  $R_{\min}$  and  $R_{\max}$  are the minimum and maximum radii, respectively,  $i_0(x) = \{[\sin(x) - x \cos(x)]/x^3\}^2$  is the sphere form factor and  $m(R) = (4\pi/3)R^3\Delta\rho$ , where  $\Delta\rho$  is the particle contrast (difference between the scattering length

density of the particle and that of the matrix). The value of  $R_{\min}$  was kept zero; that of  $R_{\max}$  was selected for each individual data set by successive runs with different values of this parameter to obtain the minimal discrepancy between the experimental and calculated scattering curves.

#### X-ray photoelectron spectroscopy (XPS)

X-ray photoelectron spectra were acquired with an Axis Ultra DLD (Kratos, UK) spectrometer using monochromatized Al K $\alpha$  (1486.6 eV) radiation at an operating power of 150 W of the X-ray tube. Survey and high-resolution spectra of appropriate core levels were recorded at pass energies of 160 and 40 eV and with step sizes of 1 and 0.1 eV, respectively. Sample area of 300  $\mu$ m  $\times$  700  $\mu$ m contributed to the spectra. The samples were mounted on a sample holder with a two-sided adhesive tape, and the spectra were collected at room temperature. The base pressure in the analytical UHV chamber of the spectrometer during measurements did not exceed 10 $^{-8}$  Torr. The energy scale of the spectrometer was calibrated to provide the following values for reference samples (i.e., metal surfaces freshly cleaned by ion bombardment): Au 4f $_{7/2}$ –83.96 eV, Cu 2p $_{3/2}$ –932.62 eV, Ag 3d $_{5/2}$ –368.21 eV. The electrostatic charging effects were compensated by using an electron neutralizer. Sample charging was corrected by referencing to the C–C/C–H peak deconvoluted in the C 1s spectrum (284.8 eV). After charge referencing, a Shirley-type background with inelastic losses was subtracted from the high-resolution spectra. The Cu and Zn LMM Auger spectra were corrected using a linear background. The surface chemical composition was calculated using atomic sensitivity factors included in the software of the spectrometer corrected for the transfer function of the instrument.

#### In vitro investigation of antifungal activity of Cu@Chit nanocomposites

The tests were performed using the agar medium assay described by Tatsadjieu et al. [20]. To evaluate the in vitro antifungal effects of the Cu@Chit NCs against *R. solani* AG2 and AG4, three concentrations of the Cu@Chit NCs suspension (30, 60, and 100 mg/L) were added to Petri dishes before pouring plates with PDA. Each Petri dish was inoculated at the center with a mycelial disc (10 mm diameter) taken at the periphery of *R. solani* colony grown on PDA at 29  $\pm$  1  $^{\circ}$ C for 3 days. Positive control (without chitosan nanocomposites) plates were inoculated following the same procedure. The growth inhibition percentage was calculated according to the formula described by Abd-El-Khair [21] which is mentioned below:

$$\text{Growth inhibition (\%)} = (C - P/C) \times 100,$$

where  $C$  is the diameter of mycelial growth in control plates, and  $P$  is the diameter of mycelial growth in treated plates. Three replicates were used per treatment, and the experiment was repeated three times. The Cu@Chit NCs with the highest levels of inhibition against the pathogens were selected for further experiments.

### Morphology of mycelia expose to Cu@Chit nanocomposites

Hyphal morphology of *R. solani* anastomosis treated with the high concentration of the Cu@Chit NCs was investigated on microscopic slides after 1 h. Morphological changes resulting from Cu@Chit-1 and Cu@Chit-2 NCs on hyphal growth were examined under light microscope (LaboMed, Los Angeles, USA). This assay enables the observation of possible morphological changes displayed by the fungus when it was exposed to Cu@Chit NCs antifungal activity. Each assay was repeated at least three times.

### Ability of *R. solani* and *S. rolfisii* isolates to produce sclerotia in vitro

One plug in diameter of 7 mm of *R. solani* and *S. rolfisii* isolates was taken for each isolate and placed in the center of a 60 mm Petri dish of PDA embedded with highest concentrations of Cu@Chit-1 NCs. Each plate was sealed with parafilm and incubated at  $25 \pm 2$  °C for 18 days. The number of sclerotia was then measured using a transparent grid with subdivisions of 5 mm<sup>2</sup>. Each subdivision with 50% or more of its area consisting of sclerotia was recorded and the number of sclerotia was calculated [22]. This procedure was replicated three times per isolate.

### Statistical analyses

Data were subjected to analysis of variance (ANOVA). Least significant difference (LSD) was used to compare concentration means within genotypes. ANOVA was performed with MSTAT-C statistical package.

## Results and discussion

In this work, the metal-vapor synthesis (MVS) was used for the preparation of copper nanoparticles which was then used for the preparation of chitosan–copper nanocomposite. According to XRF, the copper concentration (%wt) in the Cu@Chit-1 and Cu@Chit-2 is 3.7 and 5.1%, respectively. To analyze particles size and particles distribution in

polymer matrix, TEM analysis was performed. According to microphotographs (Fig. 1a, d), the particles have predominantly spherical form, polydisperse character and slightly uniform distribution in the chitosan matrix. The average particle size of metal NPs in both Cu@Chit-1 and Cu@Chit-2 composites turned out to be almost equal and was about 2–3 nm. However, TEM microphotograph of Cu@Chit-2 in the black field showed a bunch of particles in the range of 4–8 nm whereas Cu@Chit-1 exhibited some amount of large particles in the range of 10–15 nm (Fig. 1,b,e). It is worth to point out that the fraction of the large particles is higher for copper nanocomposite obtained with Cu-toluene organosol. Selected area diffraction patterns (SAED) for both composites contained rings with lattice spacings corresponded to Cu<sub>2</sub>O and Cu phase (Table 1). Thus, it can be suggested that the NCs contain copper nanoparticles covered by an overlay of copper (I) oxide which can perform protective function against further particles oxidation.

Experimental SAXS curves of Cu@Chit NCs and pristine chitosan are demonstrated in Fig. 2. The scattering curves are found to have a polydisperse character. The scattering curve for Cu@Chit-2 showed the maximal scattering intensity in very small angles ( $< 2$  nm<sup>-1</sup>). This could be explained by a higher concentration of scattering metallic particles and possibly by the presence of the larger particles or their aggregates. The second suggestion was confirmed with TEM analysis.

It should be noticed that the curves coincide in the region of scattering vector higher than 5 nm<sup>-1</sup>. Hence, the impregnation procedure of chitosan with organosol containing metallic particles has no influence on the pristine structure of polymer matrix. In this case, the scattering curve for pristine chitosan was subtracted from that of the chitosan with metal inclusions giving a curve for metallic NPs. The resulting difference curves are shown in Fig. 3.

The difference SAXS curves from Cu@Chit-1 and Cu@Chit-2 on the interval of scattering vectors from 0.4 up to about 3.0 nm<sup>-1</sup> were used to calculate volume size distribution functions  $D_V(R)$ . The applying interval limitations were caused by the necessity to exclude the influence of both the primary beam and scattering from large particles and their aggregates, which are beyond the SAXS resolution. Figure 4 demonstrates the  $D_V(R)$  for metallic particles along with the distribution function of the heterogeneities observed in pristine chitosan. The presence of heterogeneities in the pristine chitosan can be explained due to the pores or more dense regions of the polymer.

Small-angle X-ray scattering is caused by a difference in electronic densities of a scattering object and surrounding medium, i.e., by a contrast. The contrast may be either positive or negative. For the original chitosan, scattering may occur due to the pores (negative contrast) or more



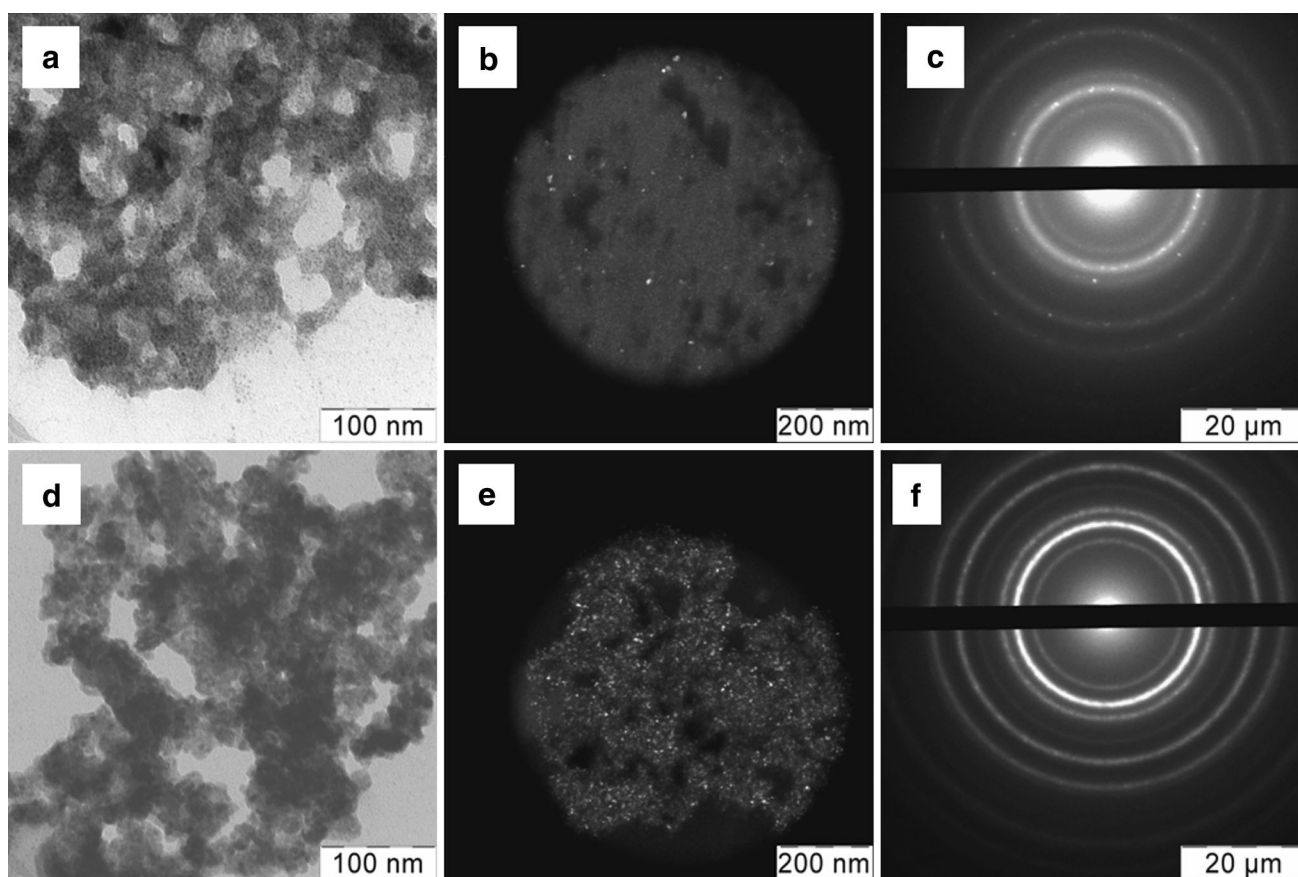


**Fig. 1** TEM microphotographs in bright (a, d) and dark field (b, e) and SAED patterns (c, f) for Cu@Chit-1 and Cu@Chit-2 NCs, respectively

**Table 1** The lattice spacings for Cu@Chit NCs determined from SAED patterns

	No.	d, Å	d, Å <sup>a</sup>	Phase
Cu@Chit-1	1	2.98	3.00	Cu <sub>2</sub> O
	2	2.42	2.45	Cu <sub>2</sub> O
	3	2.08	2.12/2.08	Cu <sub>2</sub> O/Cu
	4	1.49	1.51	Cu <sub>2</sub> O
	5	1.80	1.81	Cu
	6	1.27	1.28/1.28	Cu <sub>2</sub> O/Cu
	7	1.21	1.23	Cu <sub>2</sub> O
Cu@Chit-2	1	2.98	3.00	Cu <sub>2</sub> O
	2	2.43	2.45	Cu <sub>2</sub> O
	3	2.09	2.12/2.08	Cu <sub>2</sub> O/Cu
	4	1.80	1.81	Cu
	5	1.47	1.51	Cu <sub>2</sub> O
	6	1.26	1.28/1.28	Cu <sub>2</sub> O/Cu

<sup>a</sup> d-data taken from [23]

dense regions of the polymer (positive contrast), but the profile of the size distribution function will be the same in both cases. The coincidence of the main fraction of all

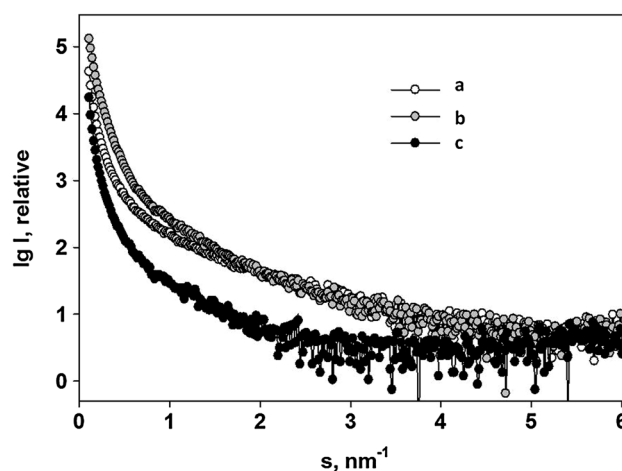


**Fig. 2** Experimental *small-angle scattering* curves for Cu@Chit-1 (a) and Cu@Chit-2 (b) NCs and pristine non-modified chitosan (c)

calculated size distribution functions reflects the fact that 2 nm metal nanoparticles most probably fill the chitosan pores with the same size. However, if for the Cu@Chit-1 fraction of the large particles is relatively small, the Cu@Chit-2 obtained with Cu-toluene organosol demonstrates much higher amount of larger NPs.

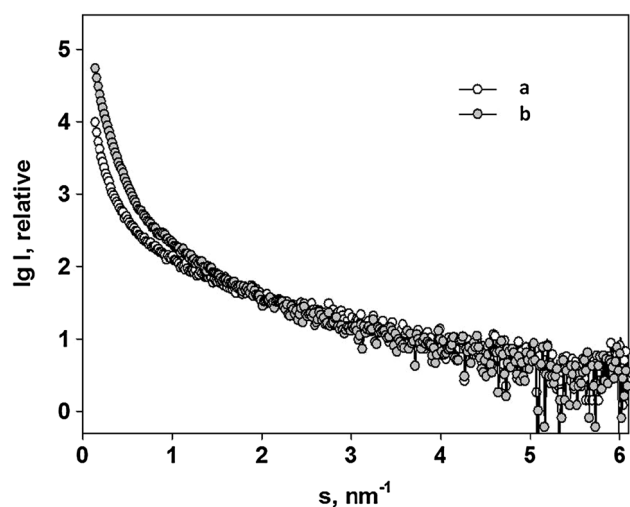


**Fig. 3** Difference small-angle scattering curves for Cu@Chit-1 (a) and Cu@Chit-2 (b) NCs

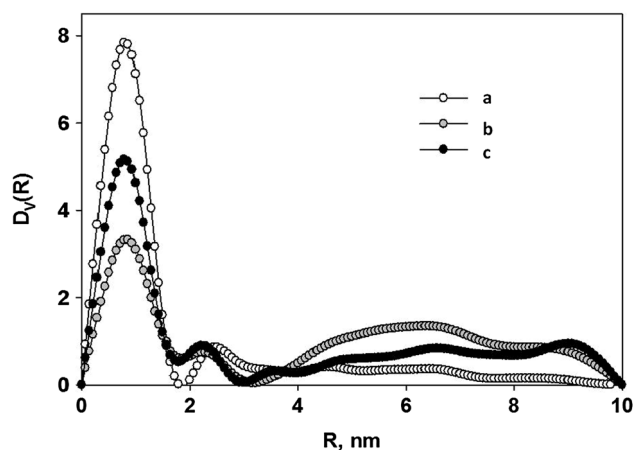


**Fig. 4** Volume size distribution function for Cu@Chit-1 (a) and Cu@Chit-2 (b) NCs and pristine non-modified chitosan (c)

**Table 2** XPS analysis of Cu@Chit NCs

Sample	Relative concentration, at. %						
	C	O	N	Cu	C/N	C/O	O/N
Chitosan	63.6	29.7	6.8	–	9.4	2.1	4.4
Cu@Chit-1	47.9	34.4	3.4	14.3	14.2	1.4	10.2
Cu@Chit-2	52.2	34.4	4.8	8.6	10.9	1.5	7.2

XPS analysis was applied for analysis of surface of the pristine and Cu@Chit NCs. It was revealed that surface composition after impregnation was changed due to slight increase of oxygen concentration while the carbon percentage decreases for the composites as compared with chitosan (Table 2). These changes are related to appearance of copper in different oxide states.

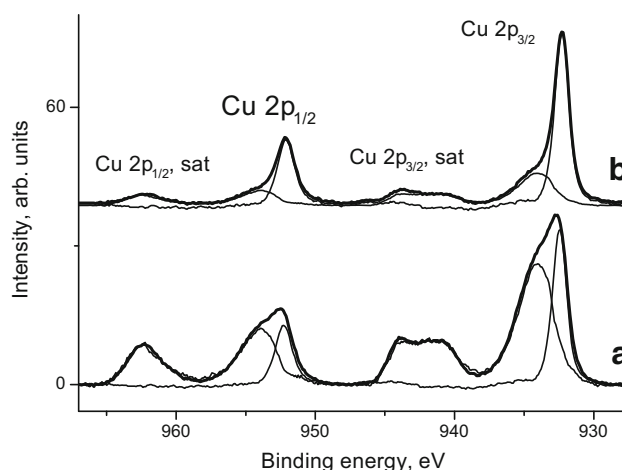


**Fig. 5** The Cu 2p photoelectron spectra for the Cu@Chit-1 (a) and Cu@Chit-2 (b) NCs normalized by intensity of the main peak

Figure 5 presents the Cu 2p photoelectron high-resolution spectra of the Cu@Chit NCs and their fitting with two states. The binding energies and Auger parameters for Cu@Chit nanocomposites are closed to each other (Table 3). It evidences similar chemical states of copper in both samples. All the spectra contained satellite peaks at binding energies about 943 and 963 eV identifying  $\text{Cu}^{2+}$  state.  $\text{Cu}^+$  state was identified according to the binding energy of the Cu  $2p_{3/2}$  peak and modified Auger parameter [24, 25]. Relative intensities of peaks determined from high resolution Cu 2p spectra are used to calculate the concentration of oxidation states of copper at surface. Thus,  $\text{Cu}^{2+}$  concentrations at the surface are 10.7 and 4.8%, whereas those of  $\text{Cu}^+$  are 3.6 and 5.5% for Cu@Chit-1 and Cu@Chit-2, respectively.

### Antifungal activity assay

The results of studies on the effect of Cu@Chit NCs on fungal growth revealed some significant inhibitory activity against two tested fungi. The effect of three concentrations of Cu@Chit NCs on mycelial growth of *R. solani* AG-4 and *S. rolfisii* is shown in Table 4.

The highest level of inhibition against *R. solani* AG-4 and *S. rolfisii* was observed using the high concentrations of Cu@Chit-1. While the lowest level of inhibition was observed using the high concentrations of Cu@Chit-2 with *R. solani* AG-4. The radial growth of *R. solani* AG-4 and *S. rolfisii* was reduced by high concentrations of Cu@Chit NCs in a dose dependent manner. The antifungal activity of the Cu@Chit NCs against *S. rolfisii* appears to be fungistatic rather than, fungicidal because growth of the fungus transferred from NCs-challenged plates to non-challenged condition was the same to growth of fungus started from untreated plates (Fig. 6). While, *R. solani* AG-4 has

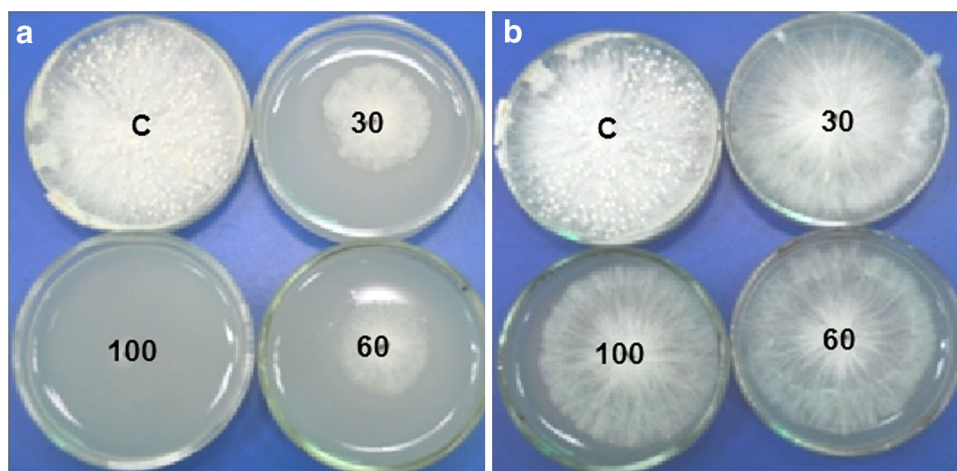


**Table 3** Binding energies of the Cu 2p photoelectron spectra and LMM Auger peaks

Sample	Cu 2p <sub>3/2</sub>	Cu 2p <sub>1/2</sub>	Cu 2p <sub>3/2</sub> , sat1	Cu 2p <sub>3/2</sub> , sat2	Cu 2p <sub>1/2</sub> , sat1	Cu LMM	Auger parameter
Cu@Chit-1	932.44	952.33	940.66	943.93	962.28	916.42	1848.86
Cu@Chit-2	932.95	952.73	941.41	944.13	962.58	916.07	1849.02

**Table 4** Mean's comparisons of in vitro antagonism of different concentrations of Cu@Chit NCs against linear growth of two sclerotium-forming plant pathogenic fungi

NCs concentrations	Sclerotium-forming fungi			
	<i>R. solani</i>		<i>S. rolfsii</i>	
	Cu@Chit-1	Cu@Chit-2	Cu@Chit-1	Cu@Chit-2
30 mg/L	1.500	0.967	4.100	0.000
60 mg/L	2.233	1.267	4.600	2.900
100 mg/L	3.267	2.467	7.033	3.100
Control	0.000	0.000	0.000	0.000
LSD ( $p < 0.05$ )	0.619	0.501	0.126	0.126

**Fig. 6** Fungicidal effect of different concentrations of Cu@Chit-1 (a) and Cu-Chit-2 (b) on mycelial growth of *S. rolfsii*

fungicidal effects in contrary with *S. rolfsii*. Since there were no significant differences in results between three concentrations of Cu@Chit NCs, more than 100 mg/L concentration was needed for antifungal activity (Table 4).

Cu–chitosan nanocomposite at 100 mg considerably hampered fungal mycelial growth and sclerotia formation in *R. solani* and *S. rolfsii*. In most cases, inhibition increased as the concentration of Chit NCs increased. This could be due to the high density at which the solution was able to saturate and cohere to fungal hyphae and to deactivate plant pathogenic fungi. The combined copper–chitosan colloids are used as a new generation of copper-based bio-pesticides [26]. Cu–chitosan has proven high antifungal activity by inhibiting spore and mycelium formation of *A. alternate*, *R. solani* and *Macrophomina phaseolina* [10, 12]. The phytopathogenic fungi usually have stronger resistance to reactive oxygen species (ROSs) attack than

bacteria or viruses, because of their much larger size and thicker cell wall/membrane. Thus, effective alternatives to chemical fungicides are difficult to develop [27].

Chitosan present in Cu–chitosan nanocomposite enhanced enzyme activities involved in plant defense. In addition, acidic environment created by the fungi in infected plant provokes the break-up of nanostructure and releases Cu ions [26]. Chitosan–Cu nanonetwork is evident through a higher Cu accumulation in porous area which supports the ion-exchange resins and surface chelating mechanism [12]. Cu–chitosan nanocomposite has a weighty effect on plant cells as they easily pass into the seeds along with encapsulated Cu and participate strongly in the metabolism of germinating seeds [13]. These studies strongly hypothesize a cumulative effect of chitosan elicitors to induce defense enzymes and direct Cu ions toxicity towards fungi.



### Effect of Cu@Chit NCs on hyphal morphology

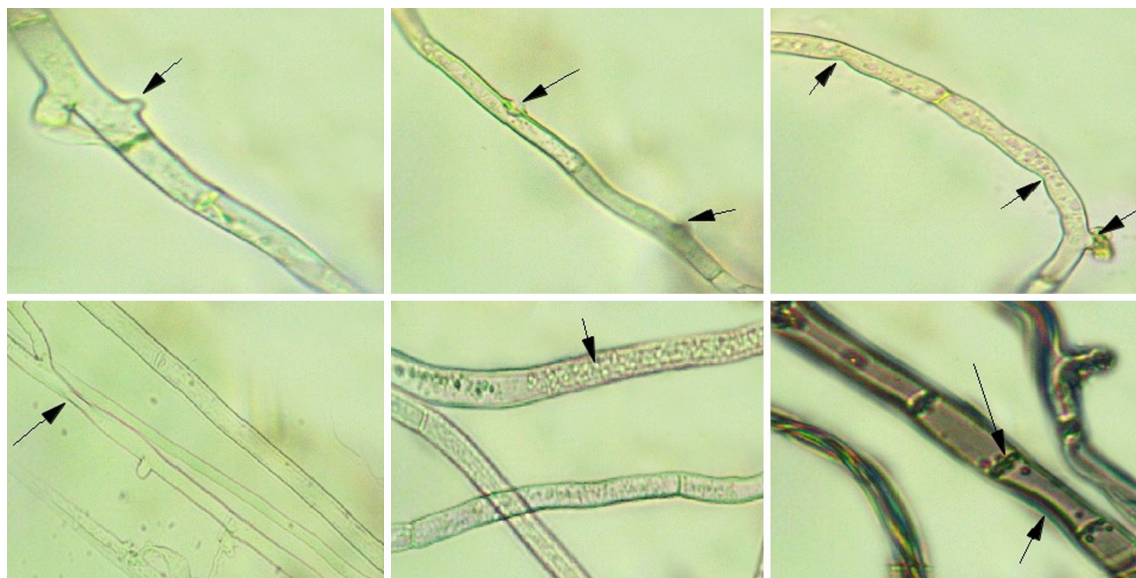
The fungal mycelia from the zone of inhibition produced by 100 mg of Cu@Chit-1 and Cu@Chit-2 NCs were observed under a light microscope (100 $\times$ ). A loss of the cytoplasm content, cytoplasmic coagulation, irregular shape of mycelia, or destruction in the hyphae was confirmed. In some cases, cell wall disruption, and consequent hyphal lysis or necrosis was detected. Upon observation, the hyphae showed mycelial deformations with swollen margins and broken mycelia, whereas the fungal mycelia from the control sample showed normal, highly branched intact morphology (Fig. 7).

However, there were other deformations such as structure of the cell membrane and inhibiting normal budding process of both *Rhizopus* sp. and *Aspergillus* sp., probably due to the destruction of the membrane integrity [28, 29]. Almost similar observation was reported by Ouda (2014) [30] who used copper and silver nanoparticles against two plant pathogens, *A. alternate* and *Botrytis cinerea*. The effects of tested Cu@Chit-1 and Cu@Chit-2 concentrations on sclerotia formation in *R. solani* AG-4 and *S. rolfsii* and was presented in Table 5. Significant differences ( $p > 0.05$ ) were observed in the number of sclerotia produced in vitro between *R. solani* treated with Cu@Chit NCs. Plates treated with 100 mg Cu@Chit NCs revealed the minimum number of sclerotia compared with control plates (Fig. 8). The highest level of inhibition against *S. rolfsii* was observed using the high concentrations of Cu@Chit-2. These results indicate that Cu-NCs strongly suppressed sclerotia formation for *R. solani* and *S. rolfsii* under in vitro condition.

### Conclusion

It is essential to develop an innovative and effective alternative nanocides such as nanometal polymer hybrids to develop new strategies for the control of sclerotium-forming plant pathogenic fungi. In this work, two Cu@Chit nanocomposites were fabricated through impregnation of chitosan with organosols Cu-acetone and Cu-toluene prepared via metal-vapor synthesis.

The particles in the nanocomposites have predominantly spherical form, polydisperse character, the mean diameter about 2–3 nm and a rather uniform distribution in the chitosan matrix. Analysis of the small angle scattering curves suggests that the copper particles in the nanocomposites with the size of  $\leq 2$  nm are mostly located in the chitosan pores with the same size. The binding energies of XPS spectra identified oxidation states of copper (I) and copper (II) for both composites; moreover, the surface of Cu@Chit nanocomposite obtained via Cu-acetone organosol is more oxidized than that of nanocomposite via Cu-toluene. Both Cu@Chit nanocomposites were examined against two plant pathogenic fungi *S. rolfsii* and *R. solani* AG-4. The results show that the Cu@Chit nanocomposites at concentration of 100 mg/L considerably hampered fungal mycelial growth and sclerotia formation in *R. solani* and *S. rolfsii*. In most cases, inhibition increased as the concentration of Cu@Chit nanocomposites increased. This could be due to the high density at which the solution was able to saturate and cohere to fungal hyphae and to deactivate plant pathogenic fungi. These results indicate that Cu@Chit nanocomposites strongly suppressed sclerotia formation for *R. solani* and *S. rolfsii* under in vitro

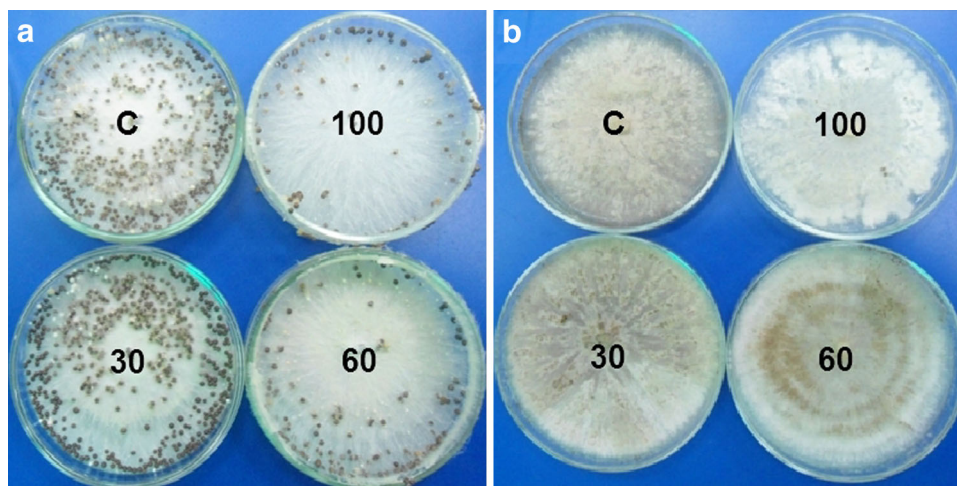


**Fig. 7** Effect of Cu@Chit-1 and Cu@Chit-2 on hyphal morphology of *R. solani* grown in PDA media. *Small arrows mark* hyphal fragmentation and cytoplasmic coagulations. *Large arrows mark* cell wall disruption and necrosis on the fungal hyphae



**Table 5** Effect of different concentrations of Cu@Chit NCs against sclerotia formation of two sclerotium-forming plant pathogenic fungi

NCs concentrations	Sclerotium-forming fungi			
	<i>R. solani</i>		<i>S. rolfisii</i>	
	Cu@Chit-1	Cu@Chit-2	Cu@Chit-1	Cu@Chit-2
100 mg/L	12.663	21.997	10.337	8.670
Control	19.100	18.997	19.100	18.997
LSD ( $p < 0.05$ )	4.228	4.854	4.228	4.854

**Fig. 8** Effect of different concentrations of Cu@Chit-1 nanocomposites on sclerotia formation of *S. rolfisii* (a), and *R. solani* AG-4 incubated at  $25 \pm 2$  °C for 18 days (b)

condition. The antifungal activity of the Cu@Chit nanocomposites against *S. rolfisii* appears to be fungistatic rather than, fungicidal because growth of the fungus transferred from NCs-challenged plates to non-challenged condition was the same to growth of fungus started from untreated plates. In the near future, production of nano-enabled fungicides with greater solubility, more stable dispersal, decreased persistence, and greater target specificity is clearly the most successful strategy for plant disease control. To the best of our knowledge, this is the first report concerning the evaluation of antifungal activity of Chit–Cu NCs developed by physico-chemical methods.

**Acknowledgment** The work is a part of the project Hybrid metal–chitosan nanocomposites: ecologically favorable synthesis, structure and plant pathogens protective properties supported by the Science and Technology Development Fund (STDF), Egypt (STDF- RFBR program) [Grant No. 13791]. Also, this work was partially funded by Russian Foundation for Basic Research grant (RFBR-15-53-61030).

**Open Access** This article is distributed under the terms of the Creative Commons Attribution 4.0 International License (<http://creativecommons.org/licenses/by/4.0/>), which permits unrestricted use, distribution, and reproduction in any medium, provided you give appropriate credit to the original author(s) and the source, provide a link to the Creative Commons license, and indicate if changes were made.

## References

1. Abd-Elsalam, K.A., Alghuthaymi, M.A.: Nanobiofungicides: are they the next-generation of fungicides? *J. Nanotech. Mater. Sci.* **2**, 1–3 (2015)
2. Abd-Elsalam, K.A., Khokhlov, A.R.: Eugenol oil nanoemulsion: antifungal activity against *Fusarium oxysporum* f. sp. *vasinfectum* and phytotoxicity on cottonseeds. *Appl. Nanosci.* **5**, 255–265 (2015)
3. Xu, J., Zhao, X., Han, X., Du, Y.: Antifungal activity of oligo-chitosan against *Phytophthora capsici* and other plant pathogenic fungi in vitro. *Pest Biochem. Physiol.* **87**, 220–228 (2007)
4. Reddy, M.V., Arul, J., Angers, P., Couture, L.: Chitosan treatment of wheat seeds induces resistance to *Fusarium graminearum* and improves seed quality. *J. Agric. Food Chem.* **47**, 1208–1216 (1999)
5. Muzzarelli, R.A.A., Muzzarelli, C., Tarsi, R., Miliani, M., Gabbanelli, F., Cartolari, M.: Fungistatic activity of modified chitosans against *Saprolegnia parasitica*. *Biomacromol* **2**, 165–169 (2001)
6. El Hadrami, A., Adam, L.R., El Hadrami, I., Daayf, F.: Chitosan in plant protection. *Mar. Drugs* **8**, 968–987 (2010)
7. Liu, H., Bao, J., Du, Y., Zhou, X., Kennedy, J.F.: Effect of ultrasonic treatment on the biochemophysical properties of chitosan. *Carbohydr. Polym.* **64**, 553–559 (2005)
8. Kruk, T., Szczepanowicz, K., Stefańska, J., Socha, R.P., Warszyński, P.: Synthesis and antimicrobial activity of monodisperse copper nanoparticles. *Colloids Surf. B* **128**, 17–22 (2015)
9. Kanhed, P., Birla, S., Gaikwad, S., Gade, A., Seabra, A.B., Rubilar, O., Duran, N., Rai, M.: In vitro antifungal efficacy of



- copper nanoparticles against selected crop pathogenic fungi. *Mater. Lett.* **115**, 13–17 (2014)
10. Saharan, V., Mehrotra, A., Khatik, R., Rawal, P., Sharma, S.S., Pal, A.: Synthesis of chitosan based nanoparticles and their in vitro evaluation against phytopathogenic fungi. *Int. J. Biol. Macromol.* **62**, 677–683 (2013)
  11. Arjunan, N., Singaravelu, C.M., Kulanthaivel, J., Kandasamy, J.: A potential photocatalytic, antimicrobial and anticancer activity of chitosan-copper nanocomposite. *Int. J. Biol. Macromol.* (2017). doi:[10.1016/j.ijbiomac.2017.03.006](https://doi.org/10.1016/j.ijbiomac.2017.03.006)
  12. Saharan, V., Sharma, G., Yadav, M., Choudhary, M.K., Sharma, S.S., Pal, A., Raliya, R., Biswas, P.: Synthesis and in vitro antifungal efficacy of Cu–chitosan nanoparticles against pathogenic fungi of tomato. *Int. J. Biol. Macromol.* **75**, 346–353 (2015)
  13. Saharan, V., Kumaraswamy, R.V., Choudhary, R.C., Kumari, S., Pal, A., Raliya, R., Biswas, P.: Cu-chitosan nanoparticles mediated sustainable approach to enhance seedling growth in maize by mobilizing reserved food. *J. Agric. Food Chem.* (2016). doi:[10.1021/acs.jafc.6b02239](https://doi.org/10.1021/acs.jafc.6b02239)
  14. Belyakova, O.A., Shuleniina, A.V., Zubavichus, Y.V., Veligzhannin, A.A., Naumkin, A.V., Vasil'kov, A.Y.: Diagnostics of gold-containing surgical-dressing materials with X-ray and synchrotron radiation. *J. Surf. Invest. X-Ray, Synchrotron Neutron Techn.* **7**, 509–514 (2013)
  15. Rubina, M.S., Kamitov, E.E., Zubavichus, Y.V., Peters, G.S., Naumkin, A.V., Suzer, S., Vasil'kov, A.Y.: Collagen-Chitosan Scaffold modifying with Au and Ag nanoparticles: synthesis, structure and properties. *Appl. Surf. Sci.* **366**, 365–371 (2016)
  16. Nikitin, L.N., Vasil'kov, A.Y., Banhero, M., Manna, L., Naumkin, A.V., Podshibikhin, V.L., Abramchuk, S.S., Buzin, M.I., Korlyukov, A.A., Khokhlov, A.R.: Composite materials for medical purposes based on polyvinylpyrrolidone modified with ketoprofen and silver nanoparticles. *Russ. J. Phys. Chem. A* **85**, 1190–1195 (2011)
  17. Vasil'kov, A.Y., Rubina, M.S., Naumkin, A.V., Zubavichus, Y.V., Belyakova, O.A., Maksimov, Y.V., Imshennik, V.K.: Metal-containing systems based on chitosan and a collagen-chitosan composite. *Russ. Chem. Bull.* **64**, 1663–1670 (2015)
  18. Konarev, P.V., Volkov, V.V., Sokolova, A.V., Koch, M.H.J., Svergun, D.I.: PRIMUS: a Windows PC-based system for small-angle scattering data analysis. *J. Appl. Crystallogr.* **36**, 1277–1282 (2003)
  19. Svergun, D.I.: Determination of the regularization parameter in indirect-transform methods using perceptual criteria. *J. Appl. Cryst.* **25**, 95–503 (1992)
  20. Tatsadjieu, L., Dongmo Jazet, P.M., Ngassoum, M.B., Etoa, F.X., Mbofung, C.M.F.: Investigations on the essential oil of *Lippia rugosa* from Cameroun for its potential use as antifungal agent against *Aspergillus flavus* Link ex Fries. *Food Cont.* **20**, 161–166 (2009)
  21. Abd-El-Khair, H., El-Gamal Nadia, G.: Effects of aqueous extracts of some plant species against *Fusarium solani* and *Rhizoctonia solani* in *Phaseolus vulgaris* plants. *Arch. Phytopathol. Plant Protect.* **44**, 1–16 (2011)
  22. Woodhall, J.W., Lees, A.K., Edwards, S.G., Jenkinson, P.: Infection of potato by *Rhizoctonia solani*: effect of anastomosis group. *Plant. Pathol.* **57**, 897–905 (2008)
  23. Hanawalt, J.D., Rinn, H.W., Frevel, L.K.: Chemical analysis by X-ray diffraction. *Ind. Eng. Chem. Anal. Ed.* **10**, 457–512 (1938)
  24. Naumkin, A.V., Kraut-Vass, A., Gaarenstroom, S.W., Powell, C.J.: NIST X-ray Photoelectron Spectroscopy Database, Version 4.1 (National Institute of Standards and Technology, Gaithersburg; <http://srdata.nist.gov/xps/>). (2012)
  25. Moretti, G.: The Wagner plot and the Auger parameter as tools to separate initial-and final-state contributions in X-ray photoemission spectroscopy. *Surf. Sci.* **618**, 3–11 (2013)
  26. Brunel, F., Gueddari, N.E., Moerschbacher, B.M.: Complexation of copper (II) with chitosan nanogels: toward control of microbial growth. *Carbohydr. Polym.* **92**, 1348–1356 (2013)
  27. Zhang, J., Liu, Y., Li, Q., Zhang, X., Shang, J.K.: Antifungal activity and mechanism of palladium-modified nitrogen doped titanium oxide photocatalyst on agricultural pathogenic fungi *Fusarium graminearum*. *ACS Appl. Mater. Interfaces.* **5**, 10953–10959 (2013). doi:[10.1021/am4031196](https://doi.org/10.1021/am4031196)
  28. Narayanan, K.B., Park, H.H.: Antifungal activity of silver nanoparticles synthesized using turnip leaf extract (*Brassica rapa* L.) against wood rotting pathogens. *Eur. J. Plant Pathol.* (2014). doi:[10.1007/s10658-014-0399-4](https://doi.org/10.1007/s10658-014-0399-4)
  29. Kim, K.J., Sung, W.S., Suh, B.K., Moon, S.K., Choi, J.S., Kim, J.G., Lee, D.G.: Antifungal activity and mode of action of silver nanoparticles on *Candida albicans*. *Biometals* **22**, 235–242 (2009)
  30. Ouda, S.M.: Antifungal activity of silver and copper nanoparticles on two plant pathogens, *Alternaria alternate* and *Botrytis cinerea*. *Res. J. Microbiol.* **9**(1), 34–42 (2014). doi:[10.3923/jm.2014.34.42](https://doi.org/10.3923/jm.2014.34.42)

